Raman amplification of ultrashort laser pulses in microcapillary plasmas

Y. Ping, I. Geltner, A. Morozov, N. J. Fisch, and S. Suckewer
Princeton University, Princeton, New Jersey 08544
(Received 23 May 2002; published 4 October 2002)

Experimental evidences of Raman amplification of ultrashort pulses in microcapillary plasmas are presented. The amplification of 100–500 fs pulses was investigated in microcapillaries with different lengths. The experimental data, together with simulation results, indicate that the resonance condition for Raman amplification in high-density plasma, $n_e \sim 1-3\times10^{20}$ cm^{-3}, existed only in a very short plasma column. Such an assumption makes it possible to reconcile the experimental results and theoretical predictions. Investigations in very short microcapillaries (0.2–0.5 mm) with a broadband seed pulse further support this hypothesis and the amplification factor is in agreement with the linear growth rate.

DOI: 10.1103/PhysRevE.66.046401 PACS number(s): 52.38.−r, 42.65.Dr, 52.50.Jm, 52.65.−y

I. INTRODUCTION

The Raman amplification is based on the three-wave interaction between two counterpropagating electromagnetic waves and a plasma wave, whose frequencies and wave vectors satisfy the energy and momentum conservation relations,

$$\omega_1=\omega_2+\omega_p,\ \vec{k}_1=\vec{k}_2+\vec{k}_p, \tag{1}$$

where $\omega_1,\omega_2,\omega_p$ are the frequencies of the pumping pulse, seed pulse, and plasma wave, respectively, and $\vec{k}_1,\vec{k}_2,\vec{k}_p$ are the corresponding wave vectors.

The idea of using Raman backscattering (RBS) as a means to amplify and compress laser pulses has been the object of study for considerable time [1–5]. Early work on the compression of laser pulses in gases was reported in Ref. [3], and recently, Raman compression from tens of nanoseconds to tens of picoseconds has been achieved in gas mixtures [5,6]. The maximum power of laser pulses that can be compressed in gases is limited by ionization. The advantage of using plasma as the medium, as recognized by Capjack *et al.* [4], is that there is no theoretical limit on the laser power since plasma can handle ultrahigh power without any ''damage'' to itself.

In order to amplify and compress laser pulses with a duration shorter than 1 ps, the bandwidth of the amplifying medium must be large enough to satisfy the Fourier relation. Early studies have recognized the difficulties of ultrashort pulse compression in plasmas because of the relatively narrow bandwidth of Raman amplification, which is the characteristic of the linear regime. In the linear regime, the intensities of the pump and the seed pulses are moderate and there is no significant pump depletion. The seed pulse grows exponentially with a growth rate, γ_{RBS}, independent of the seed intensity [7],

$$\gamma_{RBS}=a_1(\omega_1\omega_p/4)^{1/2}, \tag{2}$$

where a_1 is the normalized vector potential of the pump; $a_1=0.85\times10^{-9}\lambda_1 I_1^{1/2}$ (the pump wavelength λ_1 is in micrometer and the intensity I_1 is in W/cm^2). Theoretical investigations have shown that in the linear regime, the original weak and short seed pulse is not only amplified but also broadened in time [8]. Its front moves with the speed of light c, while its maximum moves at $c/2$, so that the amplified pulse quickly stretches to $2L_p/c$ (L_p is the plasma length) [9]. Therefore, Raman amplification in the linear regime is not very suitable for ultrashort pulses.

Recently, new effects were identified in the nonlinear behavior of plasmas when interacting with ultraintense laser pulses [10–12]. There are several mechanisms by which the pump power might be coupled into the counterpropagating seed pulse [13]: Compton scattering [10], resonant backward Raman scattering [11], and coupling at an ionization front [12]. The Compton scattering regime is also called the ''superradiant'' regime, where the electron bounce motion in the ponderomotive bucket dominates the collective oscillations of the plasma wave. The electrons behave like quasi-independent emitters and the laser pulse can be amplified through Compton scattering. This scheme requires the seed pulse to be shorter than ω_p^{-1}. In the Raman scattering regime, where a density resonance is required, it has been shown by simulations that the pulse grows so fast that it can outrun the deleterious instabilities and pump depletion can quickly take place. The efficiency could be as high as $1-\omega_p/\omega_1$. In the case of ionization-front scattering, the pump propagates through a neutral gas in order to avoid collisionless instabilities, and plasma is created in the front. In this regime, it may be necessary to employ lower pumping intensities, for instance, 10^{12} W/cm^2, which would imply that the interaction length has to be much longer than in the first two regimes to achieve the desired high output power.

Our experiments were designed initially for the linear regime with a pumping power intensity of 1×10^{13} W/cm^2. In this paper we present the results of Raman amplification in two configurations: (a) a 745-nm, 200-fs seed pulse amplified by a 5-ns, 532-nm pumping pulse in 1–3-mm-long LiF microcapillaries and (b) a broadband 500-fs pulse amplified by the same pump in copper microcapillaries (150–200 μm in diameter and 200–500 μm long). The former is a continuation of our previous work [14]. The analysis of the experimental data, together with simulation results, suggests that the observed amplification in the initial experiment was obtained from a plasma with a length much shorter than the microcapillary length. The second experiment in much shorter microcapillaries was performed to verify this hypoth-

 ©2002 The American Physical Society

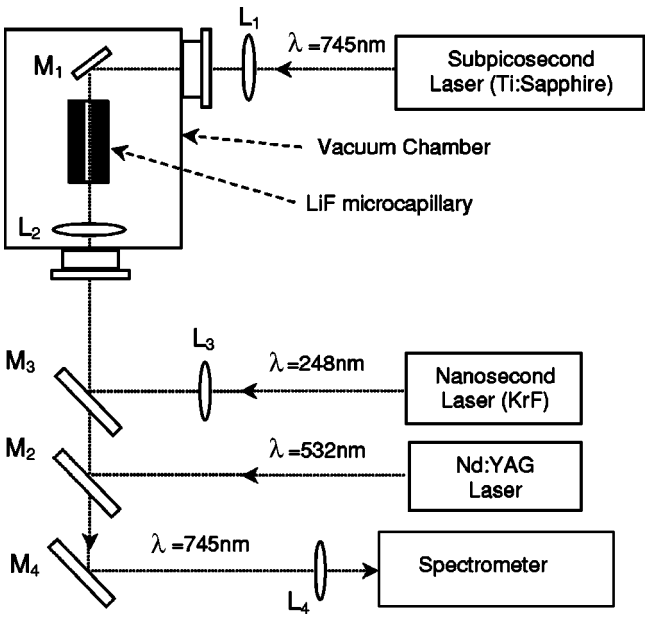

FIG. 1. Experimental setup for Raman amplification with a $\lambda = 745$ nm, 200-fs seed pulse in a LiF microcapillary.

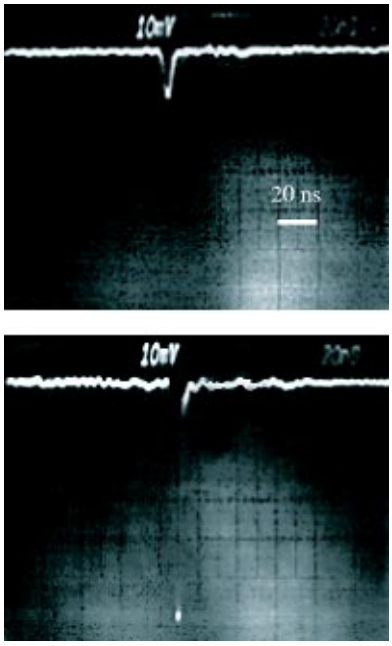

FIG. 2. Output signals of the photomultiplier without the pump (top) and with the pump (bottom) at a 40 ns delay after the prepulse ($L_{cap} = 3$ mm).

esis and the results show that the amplification agrees well with the estimated linear growth rate.

II. EXPERIMENTAL RESULTS

A. Experiments with a 745-nm, 200-fs seed pulse

In Ref. [14] we have presented, to the best of our knowledge, the first experimental results on ultrashort pulse amplification in microcapillary plasma by a counterpropagating pumping pulse. However, some of the results were difficult to interpret: the transmission of the seed pulse through the high-density 3-mm-long plasma was much higher than expected; the increment of amplification as a function of the microcapillary length was significantly less than theoretically predicted; and finally we observed the decrease of the amplification with increasing energy of the seed pulse. We present here additional experimental results, as well as amplification measurements in very short microcapillaries in the following subsection, which were helpful in better understanding the process and obtaining better agreement with the theory.

The schematic of the experimental arrangement of Ref. [14] is shown in Fig. 1. The seed pulse was the output of a Ti:sapphire regenerative amplifier at $\lambda = 745$ nm with a full width at half maximum (FWHM) of ~ 4 nm and a pulse duration of ~ 200 fs. About 30 μJ or less (of 3 mJ available) were used in the experiments. The pumping pulse was provided by the second harmonic of a Nd:YAG laser at $\lambda = 532$ nm with 150 mJ in 5 ns. The seed pulse and the pumping pulse were both focused onto the center of the microcapillary by $F/25$ and $F/8$ lenses, respectively. The initial plasma was created inside 1–3 mm long, 250-μm diameter LiF microcapillaries through wall ablation by a low power nanosecond KrF laser (50–60 mJ in 20 ns at $\lambda = 248$ nm). The amplified seed pulse, propagating in the opposite direction to the pumping pulse, was focused onto the entrance slit of a spectrometer and detected by a photomultiplier with a 2-ns time resolution.

The three-wave interaction condition for the experimental parameters, $\omega_1 = 3.54 \times 10^{15}$ rad/sec and $\omega_2 = 2.53 \times 10^{15}$ rad/sec, was satisfied by a plasma frequency $\omega_p = 1.01 \times 10^{15}$ rad/sec, corresponding to an electron density $n_e \approx 3 \times 10^{20}$ cm^{-3}. To create such a high-density plasma, we chose a LiF microcapillary with a small diameter, $D_{cap} = 250$ μm, in accordance to the estimated ablation rate of the wall [15]. The best-matched plasma density was found by scanning the delay between the prepulse and the seed pulse from 20 ns to 200 ns. The relative timing between the subpicosecond seed pulse and the pumping pulse was also finely tuned, with an accuracy of ~ 0.7 ns, in order to find the optimum conditions.

The diameters of the focal spots of the pumping pulse and the seed pulse (20 μm and 50 μm, respectively) were much smaller than the diameter of the microcapillary. The seed pulse was aligned in such a way as to have no interaction with the wall, so there was no difference in the exit energy if the microcapillary was totally removed. The pumping intensity was $\simeq 1 \times 10^{13}$ W/cm^2 and a backscattered signal was not observed at the wavelength of the seed pulse when the seed pulse was not present. Typical signals from the photomultiplier are presented in Fig. 2 without (top) and with (bottom) a pumping beam. One can see that the amplitude of the signal is increased by a factor of ~ 5 when interacting with the pumping pulse in the plasma. We have defined V_i as the signal amplitude without the pumping pulse (proportional to the total energy of the seed pulse) and V_o as the amplitude with the pumping pulse (proportional to the total energy of the amplified pulse). The amplification, V_o / V_i, as a function of the delay between the prepulse and the pumping pulse

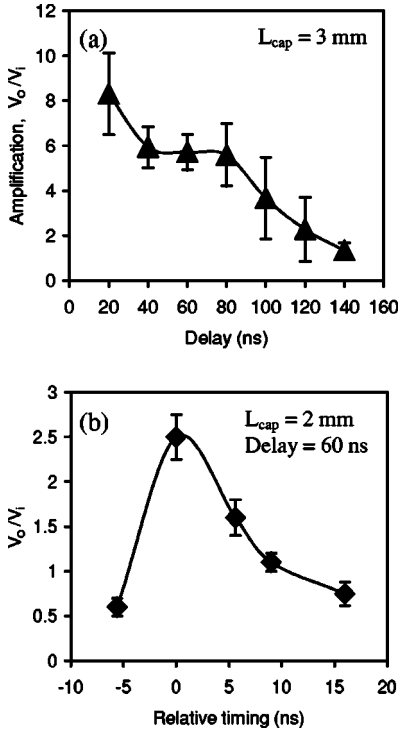

FIG. 3. (a) Amplification vs the delay between the prepulse and the pumping pulse. (b) Amplification vs the relative timing between the pumping pulse and the seed pulse (negative relative timing, "-", corresponds to the seed preceding the pump).

is shown in Fig. 3(a). The enhancement of the output signal was observed at delays between 20 ns to 120 ns. The maximum amplification (~ 8) occurs at a short delay (20 ns), but with relatively large fluctuations. From 40 ns to 80 ns there is a plateau in the amplification (~ 6) with relatively smaller spread. We performed most of the measurements at a delay of 60 ns since this was the most stable region.

Figure 3(b) shows the amplification versus the relative timing between the pumping and the seed pulses (negative relative timing, "-" corresponds to the seed preceding the pump). The optimum relative timing is defined as "0." The amplification "window" was approximately 10 ns, in agreement with the duration of the pumping pulse (FWHM 5 ns). When the seed and the pump are off in timing (<-3 ns or >10 ns) the ratio V_o/V_i drops to below 1 due to the absorption by the plasma. This "time window" agreed well with simulation results with a 1D fluid code in the radial coordinate [15]. The simulated time evolution of the plasma density with the pumping pulse fired at three different delays are presented in Fig. 4, indicating that the appropriate density was produced only when the additional ionization was induced by the pumping pulse, and only at certain delays.

In order to study the bandwidth of the amplification the spectra of the seed pulse and the amplified pulse were measured (shown in Fig. 5 for $L_{cap}=1.5$ mm, a 60 ns delay and $I_1=10^{13}$ W/cm^2). Each data point is averaged over 20 shots. It can be seen that the spectral width of the amplified pulse is only slightly narrower than that of the seed pulse, but the difference is within the measurement error. The lack of spectral narrowing could be due to density gradients, since a 3% density variation can cover the observed bandwidth.

For the 532-nm pumping pulse focused to 10^{13} W/cm^2, the vector potential is $a_1=0.0014$, therefore the growth rate, calculated by Eq. (2), is $\gamma_{RBS}\sim 1.3\times 10^{12}$ s^{-1}. If there is no energy loss and the amplification occurs through the whole Rayleigh length of the pumping beam ($Z_R\sim 0.6$ mm), for a low intensity seed pulse (no pump depletion linear regime) one would expect an amplification of $\exp(2\gamma_{RBS}Z_R/c)\sim 180$. However, given an estimated preplasma temperature T_e

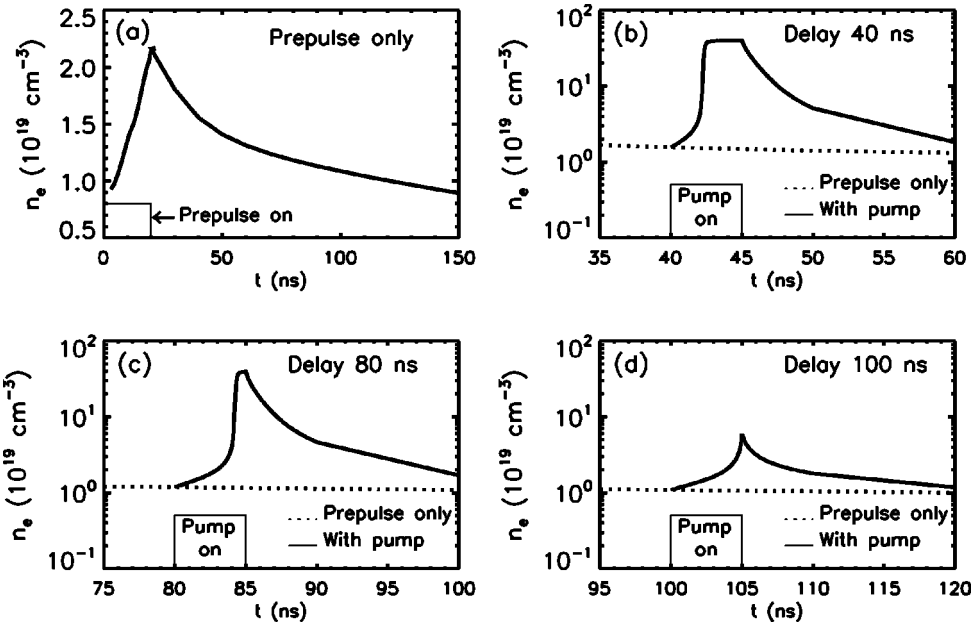

FIG. 4. Simulated time evolution of the plasma density (averaged over the central area with a radius of 20 μm) in the preplasma (a) and in the plasma heated by the pumping pulse at three delays [(b), (c), (d)]. The laser parameters are the same as in the experiment and the LiF microcapillary dimensions are $L_{cap}=3$ mm, $D_{cap}=250$ μm.

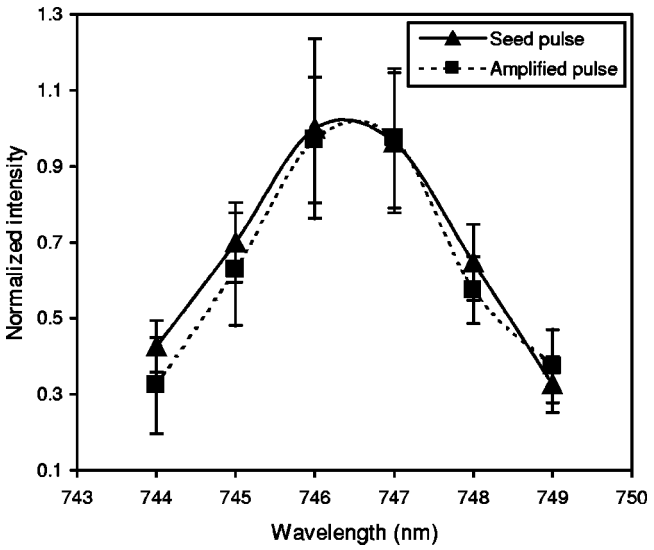

FIG. 5. Comparison of the spectra of the seed pulse (triangles) and the amplified pulse (squares). $L_{cap}=1.5$ mm, delay = 60 ns.

$\sim$20 eV and $n_e=3\times10^{20}$ cm^{-3}, the inverse Bremsstrahlung absorption length is ~100 μm, i.e., the penetration distance of the pumping pulse into the plasma is only 100–200 μm. The actual situation is more complicated since the plasma is heated and the plasma density is changed by the pumping pulse, as shown in the simulation results. In later density measurements it was found that the plasma does not fill the whole microcapillary at short delays, hence the microcapillary length is not the actual interaction length. In addition, ionization-induced defocusing, caused by additional ionization by the pumping pulse and the ensuing density profile (peaked at the center), can further limit the interaction length. If the effective interaction length is $L_{eff}\sim200$ μm, the amplification would be $\exp(2\gamma_{RBS}L_{eff}/c)\sim6$, which would be in good agreement with the observed amplification.

The short effective interaction length can also explain the decrease in the amplification with increasing seed pulse intensity [14]. During the measurement of Raman amplification as a function of seed pulse intensity (at constant pumping intensity $I_1\approx10^{13}$ W/cm^2) the amplification dropped as the intensity of the seed pulse (I_2) approached that of the pumping pulse (I_1). The explanation in view of the short L_{eff} could be as follows. The available pumping energy within the short interaction time (for $L_{eff}=0.2$ mm the interaction time is $\tau_{eff}=2L_{eff}/c\sim1.5$ ps) of the total 150 mJ in 5 ns is only ~40 μJ. When $I_2\approx I_1$, the energy of the seed pulse is ~30 μJ, which is comparable to the available pumping energy. Even with total pump depletion one cannot expect the amplification to exceed a factor of 2. While taking into account absorption and no full depletion, there should be no visible amplification. Finally, the short length of the high-density plasma can explain the high transmission of the seed pulse through the preplasma.

B. Experiment with a broadband seed in copper microcapillaries

The earlier experiments (Ref. [14] and Sec. II A) indicated that the amplification of 5–6 likely occurred in a short interaction length. In order to verify this hypothesis we conducted the experiment with much shorter microcapillaries. This allowed us to have a more precise knowledge of the interaction length. In this case the Rayleigh length of the pumping pulse ($Z_R\simeq0.6$ mm) was much longer than the microcapillary length ($L_{cap}=0.2$ mm), therefore diffraction and refraction effects were relatively insignificant. Furthermore, the development of an optical parametric oscillator (OPO, Ref. [16]), which produces a wavelength-tunable seed pulse, provided us with more freedom for matching the density.

The experimental setup was the same as in Fig. 1, except that the seed pulse was provided by the OPO, which was pumped by a 745-nm, 500-fs pulse and produced a very broadband output pulse in the visible region. The shortest wavelength that could pass through mirrors M_3 and M_4 was ~600 nm, which corresponds to a minimum matched density of $n_e=5\times10^{19}$ cm^{-3} with a 532 nm pump. The LiF microcapillaries were replaced by copper microcapillaries with lengths ranging from 200 μm to 500 μm and diameters from 100 μm to 300 μm (the usage of copper instead of LiF was due to technical difficulties in making LiF microcapillaries shorter than 1 mm). A charge-coupled device (CCD) camera was installed at the exit of the spectrometer to record the whole spectrum of the subpicosecond pulse in a single shot.

Since the spectrum intensity of the broadband seed pulse varies from shot to shot, a small portion of the seed pulse was split and focused into the spectrometer to provide a reference spectrum. Figure 6(a) displays the reference spectrum (top) and the seed pulse spectrum after passing through the empty microcapillary (bottom). In order to overcome the spatial mismatch of the seed and the pumping pulses, as encountered in the earlier experiments [14], the microcapillary was imaged at the entrance slit of the spectrometer. The related geometry is shown in Fig. 6(c). The pumping pulse was focused onto the center of the microcapillary with a spot size of ~20 μm (FWHM). The larger focal spot of the seed pulse ensured overlapping with the pumping pulse. The entrance slit of the spectrometer was 200 μm wide, which corresponds to 30 μm in the microcapillary front plane, covering the interaction area between the seed and the pump. With such an arrangement, the spectrum displayed by the CCD camera had a spectral resolution of ~0.6 nm and a spatial resolution of ~10 μm in the vertical direction [marked as the y axis in Figs. 6(b) and 6(c)].

The prepulse, for creating the preplasma inside the microcapillary, and the pumping pulse were the same as in the previous setup, i.e., about 60 mJ at 248 nm in 20 ns and 150 mJ at 532 nm in 5 ns, respectively. The spectrally resolved amplification was calculated as $S_p(\lambda)/S_0(\lambda)$, where $S_p(\lambda)$ is the intensity of the amplified pulse spectrum and $S_0(\lambda)$ is the intensity of the reference spectrum. Without the plasma the ratio S_p/S_0 was approximately a flat curve [Fig. 7(a)]. When the plasma was created in the microcapillary, the seed pulse spectrum remained almost the same, with slight spatial modifications, probably due to nonuniformities of the plasma density. When the pumping pulse was fired into the plasma, the seed pulse spectrum demonstrated a significant difference

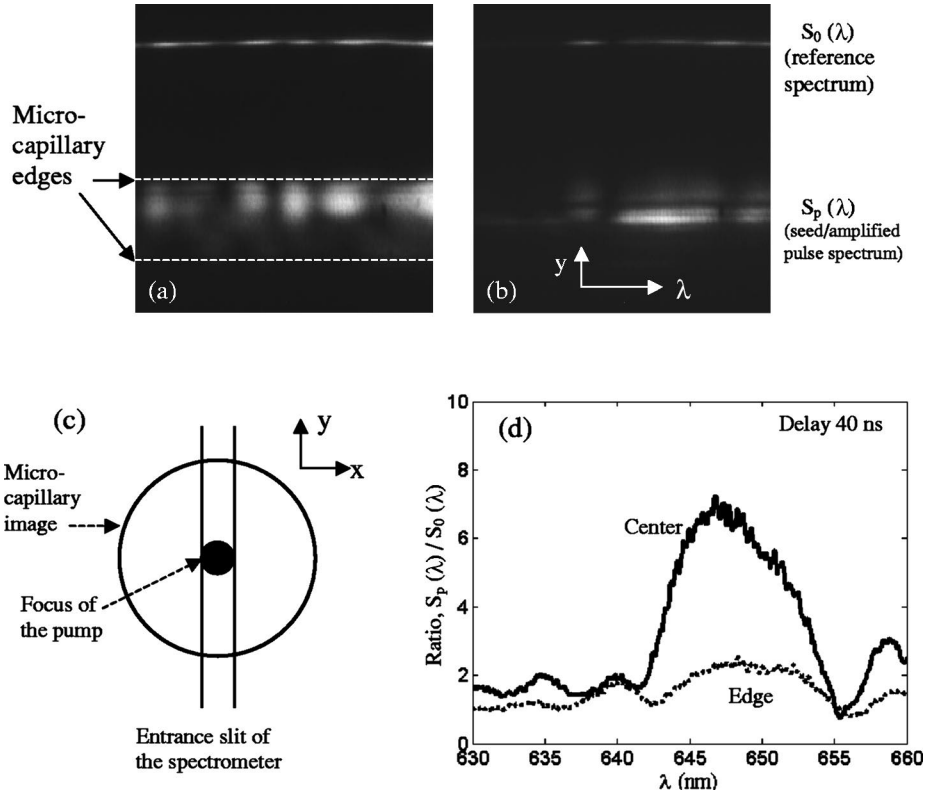

FIG. 6. (a) Reference spectrum (top, S_0) and the seed pulse spectrum (bottom, S_p). (b) Reference spectrum and the amplified pulse spectrum in a copper microcapillary with $L_{cap}=200\ \mu$m and $D_{cap}=150\ \mu$m at a delay of 40 ns. (c) Related geometry of the imaging at the entrance slit of the spectrometer. (d) Ratio of $S_p(\lambda)/S_0(\lambda)$ at the center area ($y=0$) and at the edge ($y=100\ \mu$m), both integrated over $\Delta y=30\ \mu$m, for the spectra shown in (b).

between the center, $S_p(\lambda, y=0)$, and the edge, $S_p(\lambda, y=100\ \mu\text{m})$, as shown in Fig. 6(d) ($L_{cap}=200\ \mu$m,$D_{cap}=150\ \mu$m and the delay between the prepulse and the pumping pulse was 40 ns). The ratio S_p/S_0 at the center has a distinguished peak at $\lambda=645$–650 nm with a maximum of ~ 7, while the ratio at the edge of the plasma channel is much flatter and does not exceed 2 for most wavelengths.

The amplification ratios $S_p(\lambda, y=0\ \mu\text{m})/S_0(\lambda)$ for several delays between the prepulse and the pumping pulse are shown in Fig. 7 for the same microcapillary. The horizontal coordinate has been converted from the wavelength to the corresponding plasma density, $n_e=m_e\omega_p^2/4\pi e=m_e(\omega_1-\omega_2)^2/4\pi e$. Each plot is an average of 2–3 shots. The first plot displays the ratio without the plasma. It is almost constant over the whole wavelength range, as expected. The other plots present the ratios at delays from 10 ns to 60 ns, showing a clear resonance peak at each delay. The corresponding densities of the resonance peaks are $(1.2$–$1.3)\times 10^{20}$ cm^{-3} and do not vary significantly in the time range shown. The observed maximum amplification was 3–4. The intensity of the seed pulse was below 10^{11} W/cm^2, thus there was no significant pump depletion, i.e., we were in the linear regime in this experiment. The linear growth rate of Raman backscattering was calculated to be $\gamma_{RBS}\approx 1.0\times 10^{12}$ s^{-1} for $I_1=1\times 10^{13}$ W/cm^2 and $n_e=1.3\times 10^{20}$ cm^{-3}. The amplification predicted by the linear theory for $L_{cap}=200\ \mu$m is then $\exp(2\gamma_{RBS}L_{cap}/c)\sim 3.8$, agreeing well with the experimental observation.

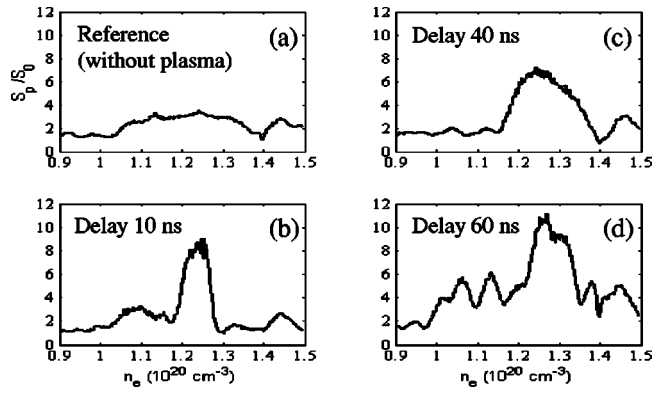

FIG. 7. The amplification ratio S_p/S_0 vs the delay between the prepulse and the pumping pulse. Each plot is an average of 2–3 shots. The horizontal coordinate is converted from the wavelength to the corresponding plasma density.

To verify the resonance density both spatial and temporal plasma density measurements were carried out [17]. The results indicate that a density of $>1\times 10^{20}$ cm^{-3} can be reached in the 200 μm microcapillaries. We also conducted the experiment with longer microcapillaries (500 μm), but it was found that due to the illumination geometry of the prepulse we could not fill the whole length with the proper plasma density.

III. CONCLUSION

In conclusion, we have shown Raman amplification of ultrashort laser pulses by a factor up to 8 in microcapillary plasmas. The analysis of the experimental data, together with simulation results, indicates that the length of the plasma with the matched density, $n_e=3\times 10^{20}$ cm^{-3}, was much shorter than the microcapillary. We conclude that due to this

short effective length the observed amplification in our initial experiment [14] was significantly less than the linear theory predicted, and the amplification dropped as the energy of the seed pulse increased since the available pumping energy within this narrow time window was very limited. Further investigations in 200-μm-long microcapillaries support the conclusion of short interaction lengths and the results show an agreement between the observed amplification and the linear growth rate.

When progressing to longer interaction lengths, spatial effects, both transversal and longitudinal, must be dealt with. In order to eliminate effects such as ionization-induced defocusing, the preplasma should be fully ionized, or at least have the next level too high for the pumping pulse to ionize. This will involve the choice of the capillary material. If the interaction length exceeds the Rayleigh length, waveguiding of the laser pulses would be required. Laser-produced plasma in microcapillaries is not suitable from this point of view. Alternative plasma-creating methods, such as discharges and laser sparks, can be employed in Raman amplification experiments.

ACKNOWLEDGMENTS

We would like to thank D. Gordon, P. Sprangle (NRL), V. Malkin (Princeton University), I. Dodin and G. M. Fraiman (Institute Applied Physics, Russia) for helpful discussions. We are also thankful to N. Tkach for excellent technical support. This work was supported by grants from DARPA and NSF (PHYS).

[1] M. Maier, W. Kaiser, and J. Giordmaine, Phys. Rev. Lett. **17**, 1275 (1966).
[2] M. Maier, W. Kaiser, and J. Giordmaine, Phys. Rev. **177**, 580 (1969).
[3] J.R. Murray, J. Goldhar, D. Eimerl, and A. Szoke, IEEE J. Quantum Electron. **15**, 342 (1979).
[4] C.E. Capjack, C.R. James, and J.N. McMullin, J. Appl. Phys. **53**, 4046 (1982).
[5] H. Nishioka, K. Kimura, K. Ueda, and H. Takuma, IEEE J. Quantum Electron. **29**, 2251 (1993).
[6] E. Takahashi, Y. Matsumoto, I. Matsushima, I. Okuda, Y. Owadano, and K. Kuwahara, Fusion Eng. Des. **44**, 133 (1999).
[7] W. Kruer, *The Physics of Laser Plasma Interaction* (Addison-Wesley, Reading, MA, 1988).
[8] D.L. Bobroff and H.A. Haus, J. Appl. Phys. **38**, 390 (1967).
[9] V.M. Malkin, G. Shvets, and N.J. Fisch, Phys. Plasmas **7**, 2232 (2000).
[10] G. Shvets, N.J. Fisch, A. Pukhov, and J.M. ter Vehn, Phys. Rev. Lett. **81**, 4879 (1998).
[11] V.M. Malkin, G. Shvets, and N.J. Fisch, Phys. Rev. Lett. **82**, 4448 (1999).
[12] V.M. Malkin and N.J. Fisch, Phys. Plasmas **8**, 4698 (2001).
[13] N.J. Fisch, V.M. Malkin, and G. Shvets, in *Superstrong Fields in Plasmas*, edited by M. Lontano, G. Mourou, O. Svelto, and T. Tajima, AIP Conf. Proc. No. **611** (AIP, Melville, NY, 2002), p. 409.
[14] Y. Ping, I. Geltner, N.J. Fisch, G. Shvets, and S. Suckewer, Phys. Rev. E **62**, R4532 (2000).
[15] A.Y. Goltsov, D.V. Korobkin, Y. Ping, and S. Suckewer, J. Opt. Soc. Am. B **17**, 868 (2000).
[16] M.K. Reed, M.K. Steinershepard, M.S. Armas, and D.K. Negus, J. Opt. Soc. Am. B **12**, 2229 (1995).
[17] Y. Ping, I. Geltner, A. Morozov, and S. Suckewer, Phys. Plasmas (to be published).